Eur. Phys. J. D **26**, 237–244 (2003)
DOI: 10.1140/epjd/e2003-00261-y

THE EUROPEAN PHYSICAL JOURNAL D

Ion trap nuclear resonance on $^{151}Eu^{+}$

S. Trapp[1], G. Tommaseo[1], G. Revalde[2], E. Stachowska[3], G. Szawiola[3], and G. Werth[1,a]

[1] Johannes Gutenberg Universität, Institut für Physik, 55099 Mainz, Germany
[2] Institute of Atomic Physics and Spectroscopy, University of Latvia, Raina Blvd. 19, Riga, Latvia
[3] Chair of Atomic Physics, Poznan University of Technology, Nieszawska 13B, 60965 Poznan, Poland

Received 7 April 2003 / Received in final form 13 June 2003
Published online 12 August 2003 –

Abstract. Laser-microwave double resonance techniques applied to a cloud of a natural mixture of Eu^{+} isotopes confined in a Penning trap has been used to induce and detect nuclear Zeeman transitions. In spite of the complex level structure of Eu^{+} and overlapping spectra from the two isotopes five different $\Delta m_I = 1$ transitions could be observed from which the nuclear magnetic moment can be derived. We obtain for $^{151}Eu^{+}$ $g_I = 1.377\,34(6)$ demonstrating the potential for high accuracy of the technique. The experiment can be considered as a feasibility test that precise spectroscopy data using the ion storage technique can be obtained of very complex ions and under unfavourable conditions.

PACS. 32.60.+i Zeeman and Stark effects – 32.10.Dk Electric and magnetic moments, polarizability

1 Introduction

Penning traps have been successfully used in recent years for high precision Zeeman spectroscopy. The long observation time under nearly perturbation free conditions impose no limit on the attainable resolution from finite observation times or collision induced line broadenings. The small volume of less than a mm^3 which an ion cloud typically occupies makes it comparatively easy to obtain a small inhomogeneity of the magnetic field inside the trap for the observation region. The first order Doppler effect plays no role in Zeeman spectroscopy since the wavelength of the radiation, typically in the mm or cm region, is much larger than the ion's oscillation amplitude in the trap. This results in a spectrum containing an unbroadened and unshifted carrier and sidebands at the ions' oscillation frequencies. Consequently high resolution in microwave induced transitions between Zeeman sublevels of electronic ground states can be achieved. With proper calibration of the magnetic field strength at the ions' position precise values of electronic magnetic moments μ can be obtained. They are usually expressed by the g_J factor defined by

$$\mu = g_J \mu_B J \tag{1}$$

where μ_B is the Bohr magneton and J is the total angular momentum quantum number. Using Penning ion traps results have been obtained on ions having electronic level structures like alkali atoms, such as Be^{+} [1], Mg^{+} [2], Ca^{+} [3], Ba^{+} [4] or Hg^{+} [5]. The strong probabilities for electric dipole resonance transitions allow easy polarization of the electronic Zeeman levels by optical pumping, and microwave induced Zeeman transitions can be detected by the change in laser induced fluorescence intensity.

Odd isotopes of these elements show hyperfine structure of the electronic ground state. In a magnetic field the Zeeman splitting depends also on the nuclear magnetic moment, and from measurements of these splittings nuclear g factors can be derived. In examples of $^{7}Be^{+}$ [6] and $^{137}Ba^{+}$ [4] ions it has been demonstrated that nuclear g factors can be determined which improve the values obtained by nuclear magnetic resonance spectroscopy in liquid or solids or on free atoms using the atomic beam resonance method. No Penning trap experiment has been described so far on ions having a more complex level structure. In this paper we report about the first attempt to perform nuclear Zeeman spectroscopy of $^{151}Eu^{+}$. The level structure of this ion shows rather high complexity: the ground state described in the L-S coupling scheme has a $4f^7 6s^9\ S_4$ configuration. The nuclear spin is $I = 5/2$ and the coupling to the electronic angular momentum leads to a complex hyperfine splitting of 6 sublevels ranging from hyperfine quantum numbers $F_{3/2}$ to $F_{13/2}$ (Fig. 1). In an external magnetic field each level is split into Zeeman sublevels. In Figure 2 the calculated energies of the ground state are plotted as function of the applied magnetic field. In the $|m_J, m_I\rangle$ coupling scheme the $|m_I\rangle$ substates within each $|m_J\rangle$ manifold range from $+5/2$ (highest energy) to $-5/2$ (lowest energy). The total number of substates is 54.

The particular interest in Eu^{+} comes from earlier measurements on the hyperfine splittings of 5 different isotopes of this element, including three unstable ones. The magnetic interaction constants $\mathcal{A}$ and the electronic

[a] e-mail: werth@mail.uni-mainz.de

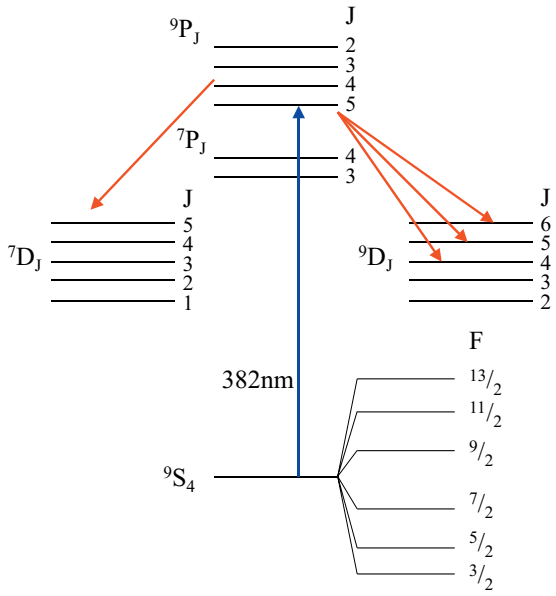

Fig. 1. Partial energy level diagram with the state $^9S_4$ for the stable isotopes $^{151}Eu^+$ and $^{153}Eu^+$.

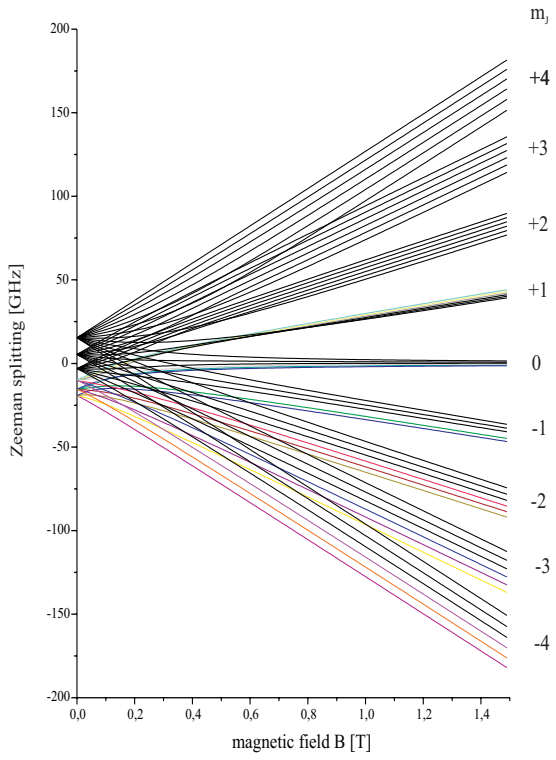

Fig. 2. Zeeman splitting of the $^9S_4$ ground state of $^{151}Eu^+$ in the presence of a magnetic field ranging up to 1.5 T.

quadrupole interaction constants $\mathcal{B}$ have been determined with a fractional uncertainty of 10^{-8} or below using microwave optical double resonance spectroscopy in a Paul trap [7–10]. For a point like nucleus the constant $\mathcal{A}$ is proportional to the nuclear magnetic moment μ_N and the magnetic field produced by the electron cloud at the nucleus which in turn is proportional to the square of the electrons wave function Ψ:

$$\mathcal{A} \propto \mu_I |\Psi|^2. \tag{2}$$

For an extended nucleus this is modified by two effects: the Breit-Rosenthal (BR) correction [12] deals with the change of Ψ due to the extended charge distribution, the Bohr-Weisskopf (BW) effect [13] describes the distribution of the magnetization over the nuclear volume. Both effects are taken into account by correction factors $(1-\varepsilon_{\mathrm{BR}})$ and $(1-\varepsilon_{\mathrm{BW}})$. While the BR correction usually is considered small, the BW effect has raised interest over many years. A recent example is the determination of the hyperfine splitting of hydrogen-like $^{209}Bi^{82+}$ [11] and $^{207}Pb^{81+}$ [14] which might be considered as a test of bound state quantum-electrodynamics. The limited knowledge of $\varepsilon_{\mathrm{BW}}$, however, leads to difficulties in the interpretation of the experimental results [15]. Generally nuclear models have provided theoretical data which in many cases do not match the experimental results [16]. Most promising for a better understanding of the BW effect would be a systematic investigation of the change in $\varepsilon_{\mathrm{BW}}$ for a series of isotopes of one element. This leads to the *differential hyperfine anomaly* $^1\Delta^2$ between two isotopes 1 and 2 defined as

$$^1\Delta^2 = \frac{\mathcal{A}_1}{\mathcal{A}_2}\frac{g_2}{g_1} \approx \varepsilon_1 - \varepsilon_2. \tag{3}$$

Typically $^1\Delta^2$ is of the order of 10^{-1}–10^{-4}. A determination of 1% then requires a knowledge of the magnetic dipole interaction constants $\mathcal{A}$ and the nuclear magnetic moments μ_N for the two isotopes of the order 10^{-3}–10^{-6}. So far the only element for which $^1\Delta^2$ has been determined experimentally for several isotopes is Hg [16]. Reasonable agreement to shell model calculations is found, the agreement is however better to an empirical model called the *Moskowitz-Lombardi rule* [17] which states that

$$\varepsilon_{\mathrm{BW}} = \frac{a}{\mu_I} \tag{4}$$

where a is an empirical constant. No theoretical justification is given for this rule. In order to check whether the agreement in the case of Hg is accidental a second investigation on a chain of isotopes would be required.

Eu seems well suited for such an investigation. Besides the two stable isotopes of mass 151 and 153 it has 6 isotopes with non-zero nuclear spin living longer than one week. Therefore this element might be subject to experiments even off the production area. Our previous experiments of the hyperfine splittings using Paul traps have demonstrated that experiments on unstable isotopes can be successfully performed. The ions have been produced by nuclear reactions at the ISOLDE/CERN facility and transported to our laboratory a the University of Mainz. The shortest living isotope which has been investigated was $^{147}Eu^+$ with a decay time of 20d. The investigation of shorter lived isotopes is possible with slight modification of the technique and of the apparatus located close to the production area. The obtained experimental uncertainty of 10^{-8} or less by far superseeds the requirements for a determination of $^1\Delta^2$.

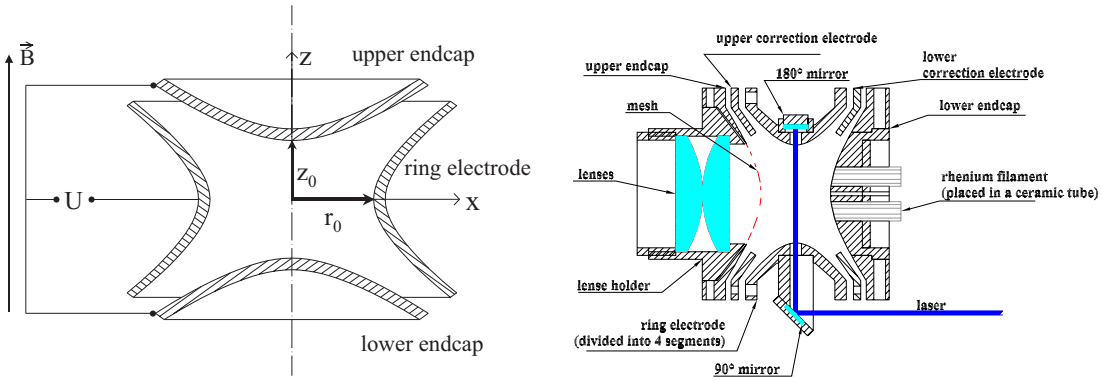

Fig. 3. Sketch of the hyperbolic Penning trap (left) and technical sketch of the Penning trap set-up used in our experiment (right).

From the theoretical side Eu isotopes ($Z = 63$) offer a one proton hole in the $5d$ proton subshell and thus can be described in the frame of a single particle model. At $N = 82$ we have a closed neutron shell. The two stable isotopes of mass 151 and 153 are a prominent example of a nuclear shape transition. This manifests itself in an exceptionally large isotope shift and in a large difference of the nuclear magnetic dipole and electric quadrupole moments [18].

Asaga and coworkers [19] have performed shell model calculations of the value of $\varepsilon_{\mathrm{BW}}$ for different Eu isotopes from which $^{1}\Delta^{2}$ can be determined. They compared their results with the predictions of the Moskowitz-Lombardi rule. In contrast to the case of Hg here the results from both predictions are rather different. Thus measurements of Eu isotopes should be a good test case for these models. The purpose of this paper is to describe a feasibility study on the determination of the nuclear magnetic moments of the same isotopes as investigated earlier using a Penning ion trap with a superimposed strong magnetic field. As mentioned above the large number of magnetic substates makes it very difficult to identify a specific state and to perform laser and microwave experiments on this state. The Doppler broadening of optical transitions in ion traps is of the order of a few GHz because of the typical kinetic energy of stored ions of a few eV. Laser cooling of Eu^{+} is not possible due to the complex electronic level structure and only moderate cooling can be obtained by collisions with a cold background gas. The nuclear Zeeman splitting which is of the order of several tenth of MHz is completely masked by the Doppler broadening. The Zeeman splitting from the electronic magnetic moment is of the same order of magnitude as the Doppler broadening and is at least partially resolved. Nevertheless we have attempted and successfully demonstrated, as shown below, that precision Zeeman spectroscopy can be performed under rather unfavourable conditions.

2 Experiment

Our Penning trap has hyperbolic shaped electrodes, one ring and two isolated endcaps (Fig. 3). It is placed in the center of a superconducting solenoid which produces a magnetic field strength of 1.4 T. A static voltage U_0 applied between the endcaps and the ring electrode produces a quadrupole potential in the space between the electrodes of the form

$$\Phi = \frac{U_0}{{r_0}^2 + 2{z_0}^2}(-r^2 + 2(z^2 - {z_0}^2)) \quad \text{with} \quad r^2 = x^2 + y^2 \tag{5}$$

r_0 is the radius of the ring electrode and is related to the distance of the two endcaps $2z_0$ by the relation $r_0 = \sqrt{2}z_0$. Our trap has the dimension $r_0 = 12.7$ mm. We keep the endcaps at d.c. ground potential and the ring is negatively charged. This allows to connect the endcaps by an inductance L. Together with the capacitance C of the trap electrodes it forms a tank circuit having a resonance frequency ω_0. This is used to detect the presence of ions in the trap: the axial oscillation frequency of an ion with charge q and mass m in the trap's potential is given by

$$\omega_z = \sqrt{-\frac{2qU_0}{m{r_0}^2}} \tag{6}$$

when the trapping voltage is ramped the ion's oscillation frequency is changed. If it matches the frequency ω_0, the ions absorb energy from the circuit. This leads to a damping of the circuit which is weakly excited at its resonance frequency. After rectification of the voltage drop across the circuit and amplification one obtains a change in the output voltage. The size of the damping depends on the quality factor Q of the circuit. A moderate value of $Q = 40$ leads to an easily detectable signal when about 10^5 ions are present in the trap. The maximum number of ions which can be trapped is limited by space charge. At typical trap voltages between 10 and 50 V this is of the order of 10^6 ions.

We load the trap with ions which are produced by surface ionisation of a metallic probe heated by a rhenium filament placed in a aperture in the lower endcap. The position of the filament approximately matches the electrode surface. A sample containing a few mg of a natural mixture of metallic europium is placed on the filament. Heating the filament for several seconds to temperatures around 1500 K produces sufficient ions to fill the trap.

The trap is placed in a vacuum vessel at a base pressure of 10^{-9} mbar. Our experiment, however, takes place at pressures of the order of 10^{-5} mbar, using N_2 as buffer gas. Collisions of the ions with the background gas serve

for different purposes: in our experiment we excite the ions by a narrow band laser from the ground state into the $^9P_5$ level for optical pumping of the ground level. As seen from the electronic level structure of Eu^+ the excited level decays back into the ground state but also partially into several metastable ^9D states (Fig. 1). The lifetime of some of these states has recently been measured to about 1 s [20]. When an ion populates one of these states it is lost from the pumping cycle until it decays back into the ground state. Collisions with neutral molecules reduce the effective lifetime to the ms range which keeps a sufficient number of ions in the pumping cycle. Moreover the ion oscillation amplitude is damped by collisions which leads to a reduced Doppler width of the optical transitions and allows a better resolution of the hyperfine structure. A problem arises with the stability of the radial orbits of the trapped ions: the ions' motion in the radial plane of a Penning trap can be described by the superposition of two harmonic oscillations at frequencies

$$\omega_+ = \frac{\omega_c}{2} + \sqrt{\frac{{\omega_c}^2}{4} - \frac{{\omega_z}^2}{2}} \tag{7}$$

$$\omega_- = \frac{\omega_c}{2} - \sqrt{\frac{{\omega_c}^2}{4} - \frac{{\omega_z}^2}{2}} \tag{8}$$

ω_+ is called the perturbed cyclotron frequency since ω_z represents only a small correction to the free cyclotron frequency $\omega_c = (e/m)B$. ω_- is the so-called magnetron frequency arising from the vector product $\mathbf{E} \times \mathbf{B}$ which describes a drift of the ions in the trap. It is a slow rotation of the ions' cyclotron orbit around the trap's center. Since the ions are attracted to the negatively charged ring electrode and only prevented by the presence of the magnetic field to move towards the ring, the magnetron oscillation can be considered as a motion around a potential hill. Perturbations of the motion by collisions would lead to a rapid increase of the magnetron radius and the ions would be lost from the trap. In fact at pressures of 10^{-5} mbar the storage time of Eu^+ is only a few seconds. This problem can be overcome by an additional radio-frequency field applied in the radial plane between adjacent segments of the ring electrode which is divided into 4 equal parts [21]. The frequency of this field is at the sum frequency of ω_+ and ω_- which is equal to the free cyclotron frequency of the ions. This field couples both motions. As shown in [22] the damping of the cyclotron motion by collisions overcomes the increase of the magnetron radius and as a consequence the ions aggregate near the trap center.

This has a number of advantages: besides the desired collisional quenching of the metastable ionic states the hot ions temperature is reduced in the buffer gas atmosphere resulting in a narrower optical line and a better spectral overlap with the exciting laser. The increased density near the trap center and the smaller ion cloud volume leads to a better spatial overlap with the laser beam. Finally the storage time is substantially enhanced, in our case typically to several days. A possible drawback is that collisional relaxation might occur between ground state sublevels which counteracts depletion by optical pumping and thus reduces the signal strength in double resonance experiments. We found, however, that the variation of the pressure by about 1 order of magnitude around 10^{-5} mbar had no significant effect on the signal strength.

2.1 Measurement of the optical and the Zeeman transitions

After storage the ions are excited from the $^9S_4$ ground state by c.w. laser radiation from a frequency doubled Ti:sapphire laser at 382 nm to the excited $^9P_5$-state. Excitation is monitored by observation of the fluorescent radiation from the excited state to the metastable $^9D_{4-6}$ states at wavelength between 630 nm and 664 nm using a broad band filter to block laser stray light. The light from the laser excited ion cloud is focussed by a lens system onto a plastic rod of 50 mm diameter and guided to a photomultiplier placed at 1.5 m distance from the trap outside the stray field of our superconducting magnet. The overall detection efficiency including solid angle, transmission losses and detector efficiency is estimated to 10^{-4}. Typical count rates are 200–500 detected photons per second at resonant excitation while the cooled GaAs photomultiplier dark counts are typically 2–4 Hz. Sweeping the laser frequency results in the observation of several resonance lines from the hyperfine and Zeeman splitting of the ground and excited state. In addition we have overlapping spectra from both stable isotopes $^{151}Eu^+$ and $^{153}Eu^+$ which have about equal abundance. In our magnetic field of 1.4 T the total span of the expected pattern has been calculated to 350 GHz (see Fig. 2). This is too much to perform a single laser scan free of mode jumps. The magnetic field is chosen as a compromise: at smaller values of the field many crossings of the Zeeman level occur as seen from Figure 2 which would make an identification of the lines very difficult. At higher values only one or two of the resonance lines would fall into the scan region of our laser of 50 GHz which would also prevent line identification. Figure 4 shows a part of the optical excitation spectrum. The peaks at the high frequency side of the spectrum have been identified as different $\Delta m_F = -1$, $\Delta m_I = 0$ transitions of the $^9S_4 - ^9P_5$ manifold of $^{151}Eu^+$ (Tab. 1).The large maximum at the center and the peaks at the low frequency side are overlapping transitions from both isotopes which could not be separated.

Optical pumping was performed by a fixed laser frequency tuned to one of the optical lines. Although the nuclear Zeeman lines are not completely resolved the Zeeman sublevels are pumped at different rates according to the Clebsch-Gordan coefficients resulting in different equilibrium populations. This was sufficient to observe a change in the fluorescence intensity when an additional radio frequency induces transitions between different nuclear Zeeman levels. The r.f. field was transmitted into the trap using the rhenium filament for the Eu^+ production as antenna. The small fluorescence signal required repetitive scanning of the microwave frequency field to obtain a signal of sufficient strength. Five different Zeeman transitions have been observed with line widths between 8 and

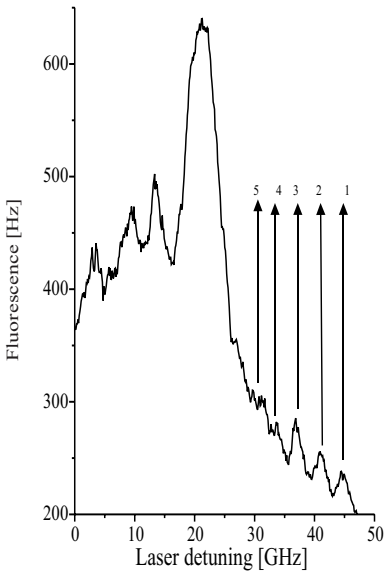

Fig. 4. Optical spectrum of the σ^+ group of $^{151,153}Eu^{+}$. The marked transitions are listed in Table 1.

Table 1. Optical transitions of the σ^+ group from the $^9S_4$ ground state to the excited $^9P_5$ state. The numbers in the first column refer to the transitions in Figure 4.

#	optical transition
1	$m_J = -4, m_I = +5/2 \longrightarrow m_J = -3, m_I = +5/2$
2	$m_J = -4, m_I = +3/2 \longrightarrow m_J = -3, m_I = +3/2$
3	$m_J = -4, m_I = +1/2 \longrightarrow m_J = -3, m_I = +1/2$
	$m_J = -3, m_I = +5/2 \longrightarrow m_J = -2, m_I = +5/2$
4	$m_J = -4, m_I = -1/2 \longrightarrow m_J = -3, m_I = -1/2$
	$m_J = -3, m_I = +3/2 \longrightarrow m_J = -2, m_I = +3/2$
5	$m_J = -4, m_I = -3/2 \longrightarrow m_J = -3, m_I = -3/2$

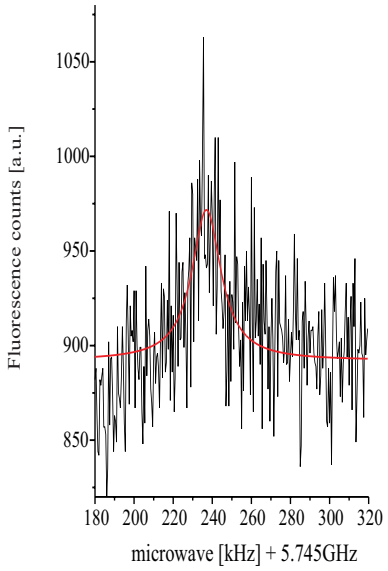

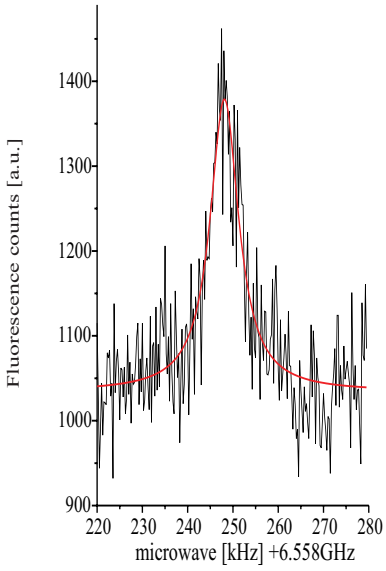

Fig. 5. Examples of observed nuclear Zeeman transitions with fitted Lorentzian line shapes. The resonance on the left hand side corresponds to the transition $m_J = -4$, $m_I = -3/2 \rightarrow m_I = -1/2$ whereas the resonance on the right hand side corresponds to the transition $m_J = -4$, $m_I = 3/2 \rightarrow m_I = 5/2$. The complete list of observed transitions is given in Table 2.

17 kHz. They are least squares fitted to Lorentzian line shapes and the line center could be determined to about 1 kHz or less. Figure 5 shows as examples the two transitions having the largest and the smallest signal strength. The measured transition frequencies are listed in Table 2.

2.2 Calibration of the magnetic field

The calibration of the magnetic field is performed by the cyclotron frequency of electrons stored in the same trap, after reversing the sign of the trapping voltage. About 10^4 electrons emitted from a hot tungsten wire at 10 cm distance from the trap are stored and detected in a similar way as described for the Eu^{+} ions by a damping signal of an attached resonant circuit. The damping arises from induced currents in the endcap electrodes by the electrons'

Table 2. List of the induced $\Delta m_I = +1$ Zeeman transitions which were observed in our experiment.

transition	ν [kHz]	$\Delta\nu$ [kHz]	FWHM [kHz]	$\Delta\nu/\nu$
$m_J = -4;\ m_I = +3/2$ $\rightarrow +5/2$	6 558 248.1	0.4	7.7	5.6×10^{-8}
$m_J = -4;\ m_I = +1/2$ $\rightarrow +3/2$	6 241 411.5	1.0	11.0	1.6×10^{-7}
$m_J = -4;\ m_I = -1/2$ $\rightarrow +1/2$	5 975 525.7	0.8	11.9	1.3×10^{-7}
$m_J = -4;\ m_I = -3/2$ $\rightarrow -1/2$	5 745 237.0	0.9	16.7	1.5×10^{-7}
$m_J = -3;\ m_I = +3/2$ $\rightarrow +5/2$	5 642 485.1	0.7	11.1	1.2×10^{-7}

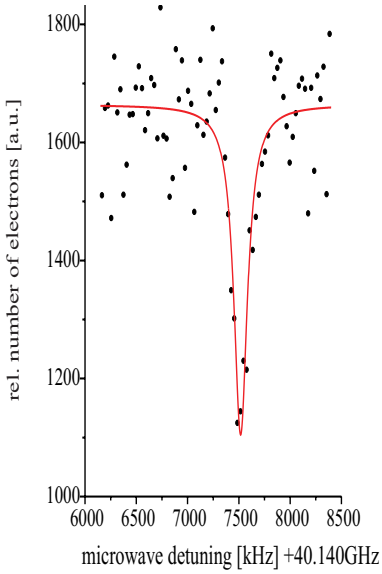

Fig. 6. Cyclotron resonance of stored electrons for calibration of the magnetic field. The full width at half maximum (FWHM) is 134 kHz and the statistical uncertainty of the center frequency is 6.5 kHz corresponding to $\delta\nu/\nu = 1.5 \times 10^{-7}$.

axial oscillation at a frequency of 12.4 MHz at a trapping voltage of 6 V.

The microwaves at the cyclotron frequency of around 40 GHz are guided into the apparatus to the trap through a semiflexible cable. When the frequency of the microwave field matches the cyclotron resonance, the electrons gain energy and some of them are lost from the trap. The reduction in signal height serves to monitor the cyclotron frequency. Figure 6 shows a typical example of a cyclotron signal from which the magnetic field was determined with an uncertainty of 1.5×10^{-7}. Measurements of the magnetic field strength have been performed before and after the observation of Zeeman resonances on Eu^+ and the average value was taken for the evaluation. We observed drifts of the magnetic field at a rate of about 10^{-8} per hour. Since the averaging time for the Zeeman resonances in Eu^+ was typically less than 20 min the drift has no influence on the result. Switching the polarity of the trap voltage for storage of either electrons or Eu^+ ions may be a source of error when the electric center of the trap is not the same for both particles as a result of contact potentials. Then electrons and ions may not see the same magnetic field if inhomogeneities are present. To check this effect we applied a bias voltage between the trap's endcap electrodes and thus shifted the center of the electron cloud by about 3 mm. No systematic change of the cyclotron frequency was observed and we consider this effect negligible.

3 Data evaluation and results

The method of the determination of g_I from experimental Zeeman splittings is based on diagonalization of the zero field hyperfine- and Zeeman-interaction energy matrix,

Table 3. Hyperfine energy separations in the $^9S_4$ ground state of $^{151}Eu^+$ derived from measurements reported in [7]. Zero energy is set at the center of the hyperfine pattern.

Hyperfine substate	E_{HFS}[kHz]
$F = 13/2$	15 402 780.639
$F = 11/2$	5 385 337.811
$F = 9/2$	–3 087 806.310
$F = 7/2$	–10 018 230.989
$F = 5/2$	–15 407 226.710
$F = 3/2$	–1 925 594.728

where g_I is treated as an adjustable parameter. The nuclear spin of $I = 5/2$ gives rise to a total of 54 Zeeman sublevels. The diagonal energy matrix elements in IJ-coupling refer to the energies of the hyperfine levels in zero magnetic field and the diagonal part of the Zeeman effect. The hyperfine levels are well-known from earlier precise measurements on the hyperfine splittings in a Paul trap [7]. They are listed in Table 3.

The diagonal matrix elements of the Zeeman effect can be calculated according to

$$\langle \alpha JIFm_F|\mathcal{H}_{\mathrm{Zeeman}}|\alpha JIFm_F\rangle = \mu_B B m_F g_F \tag{9}$$

with

$$g_F \equiv g_J \frac{F(F+1)+J(J+1)-I(I+1)}{2F(F+1)} - g_I \frac{\mu_K}{\mu_B} \frac{F(F+1)+I(I+1)-J(J+1)}{2F(F+1)}. \tag{10}$$

The non-diagonal elements are given by

$$\langle \alpha JIFm_F|\mathcal{H}_{\mathrm{Zeeman}}|\alpha JI(F-1)m_F\rangle = g_J\mu_B B \times \sqrt{(F+m_F)(F-m_F)} \times \sqrt{\frac{(I+J+F+1)(I+F-J)(J+F-I)(I+J+1-F)}{4F^2(2F+1)(2F-1)}} \times \left(1+\frac{g_I}{g_J}\frac{\mu_K}{\mu_B}\right) \tag{11}$$

using

$$\langle \alpha JIFm_F|\mathcal{H}_{\mathrm{Zeeman}}|\alpha JIF'm_F\rangle = \mu_B B(-1)^{F-m_F} \begin{pmatrix} F & 1 & F' \\ -m_F & 0 & m_F \end{pmatrix} \times g_J \{\langle \alpha JIF||J_z||\alpha JIF\rangle - \gamma \langle \alpha JIF||I_z||\alpha JIF\rangle\} \tag{12}$$

with

$$\gamma \equiv \frac{g_I}{g_J}\frac{\mu_K}{\mu_B}. \tag{13}$$

The energy matrix is then numerically diagonalized assuming a value for g_J, obtained using wave function from a semiempirical method: the intermediate wave function can be written as a linear combination of pure LS-states:

$$\Psi = \sum_{i=1}^{n} \alpha_i |LS\rangle_i. \tag{14}$$

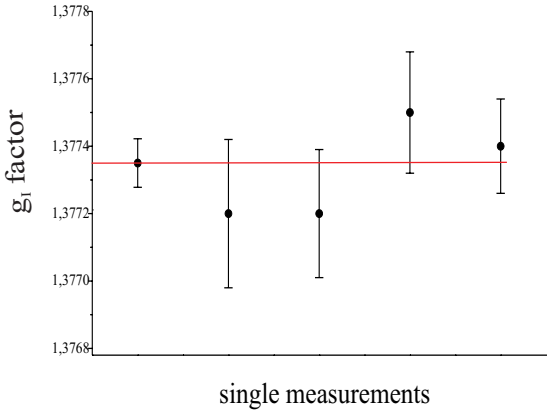

Fig. 7. The values for the nuclear g_I factor resulting from the five single Zeeman transitions listed in Table 2.

The normalized coefficients α_i are determined in a self consistent Hartree-Fock approximation: the hyperfine coupling parameters and the coefficients are adjusted in such a way that the deviation from the experimentally obtained hyperfine splittings are minimized. This procedure has been described in detail in [7,10] and leads to the following wavefunction:

$$\begin{aligned}
&|4f^7(^8\mathrm{S})6s;\,^9\mathrm{S}_4\rangle = \\
&\quad +0.984145|4f^7(^8\mathrm{S})6s;\,^9\mathrm{S}_4\rangle + 0.175147|4f^7(^6\mathrm{P})6s;\,^7\mathrm{P}_4\rangle \\
&\quad -0.003930|4f^7(^6\mathrm{D})6s;\,^5\mathrm{D}_4\rangle - 0.014394|4f^7(^6\mathrm{D})6s;\,^7\mathrm{D}_4\rangle \\
&\quad +0.000559|4f^7(^6\mathrm{F})6s;\,^5\mathrm{F}_4\rangle \\
&\quad +0.001220|4f^7(^6\mathrm{F})6s;\,^7\mathrm{F}_4\rangle + \ldots \qquad (15)
\end{aligned}$$

Using this wavefunction the g_J for the ground state can be determined to:

$$g_J(\Psi) = \sum_{i=1}^{n} {\alpha_i}^2 g_J^{(i)}. \qquad (16)$$

The value which we obtain is

$$g_J = 1.991\,169. \qquad (17)$$

Substituting this value to the energy matrix, g_I remaining as the only free parameter, is varied to minimize the difference between the calculated and observed Zeeman intervals for a given $\Delta m_J = 0$, $\Delta m_I = 1$ transition. The results of this procedure are shown in Figure 7. The values of g_I from the different observed transitions agree with each other within their limits of error. As weighted average we obtain:

$$g_I = 1.377\,34(6). \qquad (18)$$

4 Discussion

In spite of a number of experimental difficulties arising from the very complex level structure of Eu^+ it has been demonstrated that even under unfavorable conditions the method of Zeeman spectroscopy in a Penning trap can produce results which are at least comparable to other methods. The value of the nuclear magnetic moment for $^{151}Eu^+$ is about a factor of 3 more precise than the previously known best value. Evans *et al.* [23] used the atomic beam resonance method (ABMR) on neutral ^{151}Eu and obtained $g_I = 1.375\,6(2)$ (without diamagnetic correction). Our result is in slight disagreement with this value. This may be due to uncertainties in the calculated g_J factor (Eq. (17)). We would like to point out, however, that terms depending on the g_J factor usually contribute in first order to the energy of the Zeeman sublevels. In this study only microwave transitions with $\Delta m_J = 0$ were measured (see Tab. 2). Therefore the contributions from those terms disappear in first order and contribute only in second order. As a consequence the terms with g_I dominate the splitting of the sublevels. The fact that our experiment produced the same value for μ_I from 5 different transitions gives confidence in our method, particularly since the complex matrix diagonalization prevents linear dependence of the different transitions.

Further improvements seem possible: obviously the use of separated isotopes would avoid one of the complications. The method described previously to accumulate the ions near the trap center by coupling the magnetron and cyclotron motion is in principle well suited. The frequency $\omega_c = \omega_+ + \omega_-$ which is used to drive the ions into the trap center depends on the mass m and on the charge e of the particle:

$$\omega_c = \frac{e}{m} B. \qquad (19)$$

Consequently one would expect that at the proper frequency only one of the two isotopes would aggregate at the trap center while the other isotope would be destabilized by collisions. In fact it has been reported that even isobars could be separated by this method [24]. In these experiments, however, single or very few particles have been used. In our cloud of about 10^5 ions the overlap of the two isotopes leads to a strong coupling and the Coulomb interaction makes it impossible to separate them. Several attempts to apply this method of isotope separation varying the buffer gas pressure and the coupling field amplitude remained unsuccessful.

A weakness of the evaluation process is that we have to assume a theoretical value for the electronic g_J factor, although its value has been derived from wavefunctions used for hyperfine analysis of very precise measurements. It would be preferable to obtain independently an experimental value in order to check the theoretical procedure. This could be done in experiments on a Eu^+ isotope with zero nuclear spin such as $^{148}Eu^+$. The lifetime of this isotope of $54d$ would allow a similar experiment as described above with little modifications.

To take however fully advantage of the accuracy in our measurements some additional effects should be taken into account, particularly all contributions originating from zero-field hfs interaction. This means that the diagonalization process should involve not only $\mathcal{A}$ and $\mathcal{B}$ hfs constants related to the hfs energy matrix elements, diagonal

with respect to $IJFm_F$ quantum numbers, but also off-diagonal elements, responsible for J-breaking as a good quantum number. The best solution is to follow a similar procedure as it was proposed for neutral europium [25]. However, the secular equations should be enriched with off-diagonal hfs electric quadrupole constants because of the challenge to approach the precision of the experimental results as given in (Tab. 2) and to improve the accuracy of the g_I determination. The problem of J-breaking in hfs of europium ions has been solved to some extent in [7], where it has been shown that particularly hyperfine sublevels of the $^9S_4$ state are strongly perturbed mainly by the sublevels of the $^7S_3$ state. In the mentioned paper the corresponding second order contribution to the hfs was estimated in an iterative procedure and the resulting correction of the $\mathcal{B}$-value amounts to a few MHz. However this approach in accounting for second order hfs perturbation can not be straightforward applied here because of the presence of the magnetic field. In this case it would be necessary to take into account also the second order hfs-Zeeman correlated term:

$$\begin{aligned}\delta W_{\mathrm{hfs-Zeeman}}(\alpha, IJFm_F) = \\ \langle \alpha, IJFm_F | \mathcal{H}_{\mathrm{hfs}} | \alpha', IJ'Fm_F \rangle \\ \times \frac{\langle \alpha', IJ'Fm_F | \mathcal{H}_{\mathrm{Zeeman}} | \alpha, IJ'F'm_F \rangle}{E(\alpha, JFm_F) - E(\alpha', J'Fm_F)} \\ + \langle \alpha, IJFm_F | \mathcal{H}_{\mathrm{Zeeman}} | \alpha', IJF'm_F \rangle \\ \times \frac{\langle \alpha', IJF'm_F | \mathcal{H}_{\mathrm{hfs}} | \alpha, IJ'F'm_F \rangle}{E(\alpha, JFm_F) - E(\alpha', J'Fm_F)}. \quad (20)\end{aligned}$$

However, calculations of hfs and Zeeman second order corrections suffer from the same weakness as the theoretical determination of g_J, because of the requirement of very accurate intermediate wave functions. Pointing at the high experimental precision, a method directly accounting for second order perturbations by diagonalization of the energy matrix containing off-diagonal hfs constants would be more adequate.

It is necessary to remember that the zero-field hfs operators preserve F and the resultant $m_F = m_I + m_J$ as good quantum numbers (J-breaking) whereas operators representing atom-magnetic field interaction preserve m_F while F is broken. This indicates that the basis for diagonalizing the hfs matrix is not identical with that for the Zeeman effect. Thus assuming $|m_I m_J\rangle$ states which are convenient to designate Zeeman sublevels at 1.5 T magnetic field strength as initial basis, the hfs matrix has to be transformed from the $|Fm_F\rangle$ representation to the appropriate one in the $|m_I m_J\rangle$ representation. To perform this it is necessary to know the explicit form of the hfs energy matrix with off-diagonal matrix elements (with respect to J), which involve off-diagonal hfs constants as parameters.

Unfortunately the absolute differences between hfs sublevels of the ground and perturbing states in $^{151}Eu^+$ are measured only with optical interferometric precision and thus far from requirements. Moreover in the case under study, in a simultaneously determination of the diagonal and off-diagonal hfs constants in a least-square fitting procedure the angular coefficients fall into quasi-linear dependencies making their correct determination impossible.

Refining the g_I and g_J factors from the measured Zeeman splitting caused by magnetic field of intermediate magnitude at 1.5 T the possible decoupling of total orbital angular momentum L and total momentum spin S should be considered. This decoupling may lead to the significant second order perturbation of pure Zeeman origin even from the perturbating levels of different J quantum number. Particularly in this way the sublevels of the $^9S_4$ state can be perturbed by the $^7S_3$-level.

In summary our study on the possibility to determine experimentally the nuclear magnetic moment of Eu^+ ions stored in a Penning trap has been successful. Additional theoretical work is necessary to fully exploit the experimental precision. The investigation of a chain of stable and unstable isotopes as previously performed in a Paul trap for hyperfine measurements seems feasible. This would lead to accurate values for the differential hyperfine anomaly for a chain of isotopes. Unstable isotopes can be produced in sufficient quantities at the ISOLDE facility at CERN, moreover in isotopically pure form.

We gratefully acknowledge a grant from the Deutsche Forschungsgemeinschaft. G.R. acknowledges support by the Fritz-Thyssen-Foundation. A part of the work was supported in the frame of a DS-project by Poznan University of Technology.

References

1. D.J. Wineland *et al.*, Phys. Rev. Lett. **50**, 628 (1983)
2. J.J. Bollinger *et al.*, Bull. Am. Phys. Soc. **37**(3), 1117 (1992)
3. G. Tommaseo *et al.*, Eur. Phys. J. D **25**, 113 (2003)
4. G. Marx *et al.*, Eur. Phys. J. D **4**, 279 (1998)
5. W. Itano *et al.*, J. Opt. Soc. Am. B **2**, 1352 (1985)
6. J.J. Bollinger *et al.*, *Laser Spectroscopy VI*, edited by H.P. Weber, W. Luthy (Springer Verlag, Heidelberg, 1983)
7. O. Becker *et al.*, Phys. Rev. A **48**, 3546 (1993)
8. K. Enders *et al.*, Phys. Rev. A **52**, 4434 (1995)
9. K. Enders *et al.*, Z. Phys. D **42**, 171 (1997)
10. K. Enders *et al.*, Phys. Rev. A **56**, 265 (1997)
11. I. Klaft *et al.*, Phys. Rev. Lett. **73**, 2425 (1994)
12. E. Rosenthal, G. Breit, Phys. Rev. **41**, 459 (1932)
13. A. Bohr, V.W. Weisskopf, Phys. Rev. **77**, 94 (1958)
14. P. Seelig *et al.*, Phys. Rev. Lett. **81**, 4824 (1998)
15. T. Kühl *et al.*, Nucl. Phys. A **626**, 235 (1997)
16. S. Büttgenbach, *Hyperfine Structure in 4d- and 5d-Shell Atoms*, Springer Tracts in Mod. Phys. (Springer, Berlin, 1982), Vol. 96
17. P.A. Moskowitz, M. Lombardi, Phys. Lett. B **46**, 334 (1973)
18. S.A. Ahmad *et al.*, Z. Phys. A **321**, 35 (1985)
19. T. Asaga *et al.*, Z. Phys. A **359**, 237 (1997)
20. D. Rostohar *et al.*, Phys. Scripta **64**, 237 (2001)
21. G. Savard *et al.*, Phys. Lett. A **158**, 247 (1991)
22. C. Lichtenberg *et al.*, Eur. Phys. J. D **2**, 29 (1998)
23. L. Evans *et al.*, Proc. Roy. Soc. A **289**, 114 (1966)
24. H. Raimbault-Hartmann *et al.*, Nucl. Instr. Meth. B **126**, 378 (1997)
25. H.-D. Kronfeldt *et al.*, Phys. Rev. A **44**, 5737 (1991)